

Improvements in ultra-high precision surface structuring using synchronized galvo or polygon scanner with a laser system in MOPA arrangement

M. Zimmermann^{*a}, B. Jaeggi^b, B. Neuenschwander^b,

^aBern University of Applied Sciences, Institute for Mechatronic Systems, Pestalozzistrasse 20,
CH-3400 Burgdorf, Switzerland

^bBern University of Applied Sciences, Institute for Applied Laser, Photonics and Surface
Technologies, Pestalozzistrasse 20, CH-3400 Burgdorf, Switzerland

ABSTRACT

In earlier work the capabilities of synchronizing a galvo scanner or a polygon line scanner with a picosecond laser system in MOPA arrangement were presented. However these systems only enabled precise positioning of laser pulses on the target relatively to each other. Since then a novel approach to increase the absolute precision in positioning has been developed. This improvement enables new and more efficient process strategies such as bidirectional processing or high precision structuring of large areas in combination with additional mechanical axes. These improvements represent a major step towards large scale industrial applications in laser based micromachining.

Keywords: ps-Pulses, Galvo Scanner, Synchronized Mode, Micromachining, High Repetition Rates, High Average Power, MOPA arrangement

1. INTRODUCTION

Picosecond laser micromachining is an interesting solution for high precision surface structuring. According to the publications¹⁻⁴ the optimal pulse energy depends on the spot radius and the threshold fluence of the processed material. Hence an efficient increase of the material removal rate is only possible by increasing the pulse repetition frequency. Furthermore for a minimized surface roughness the pitch, which means the distance between two consecutive pulses, should be half of the spot radius w_0 ⁴. In consequence higher removal rates at an optimal surface roughness directly imply increased scanner velocities. Therefore polygon mirror line scanners⁵ with scanning velocities in the range of 100m/s are of great interest. However one of the drawbacks of polygon line scanners is their fixed line length. So if the biggest dimension of a machined structure is significantly smaller than the nominal line length of the polygon line scanner the duty cycle of laser processing is also significantly reduced. From this point of view recent developments prove that a synchronized galvo scanner machining is still an interesting solution when dealing with small and variable sized work pieces.

The laser system used for all experiments was a FUEGO from Time Bandwidth Products equipped with a frequency conversion and a pulse on demand module, which delivers single pulses up to approximately 2.5MHz at 1064nm wavelength. All scanners used were IntelliScan_{DE}14 from Scanlab controlled by RTC5 scanner controller boards

2. SYNCHRONIZED OPERATION

The pulse repetition frequency (*PRF*) of laser systems with a passive mode-locked seed laser in a master oscillator power amplifier (MOPA) arrangement is an integer fraction of the constant master oscillator frequency. For surface structuring the beam of laser pulses is distributed on a target with mechanical deflection systems such as galvanometric or polygon scanners. These deflection systems are governed by numerical controllers with their specific controller clock frequency (*CCF*). The clock derivation depicted in figure 1 enables synchronization of the *CCF* with an integer fraction of the *PRF*.

*markus.zimmermann.1@bfh.ch; phone +41 (0)34 426 43 56

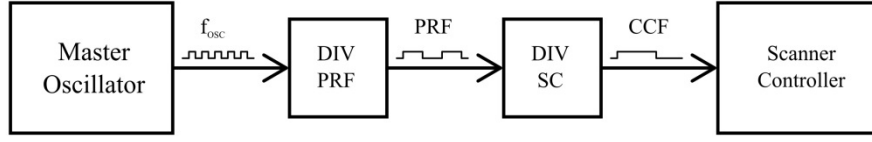


Figure 1. Configuration of clock derivation for synchronized scanner controller operation.

As presented in⁴ synchronized controller clock enables very accurate raster scanning. The difference between unsynchronized and synchronized operation is depicted in figure 2. Figure 2a represents a typical machining pattern in unsynchronized mode with lines processed in positive x-direction. The frequency deviation between the *PRF* and the *CCF* in unsynchronized mode leads to a jitter in the starting positions of the lines in x-direction. As shown on figure 2b synchronization eliminates the jitter of the starting positions in x-direction and consequently each horizontal line starts exactly at the same x-position.

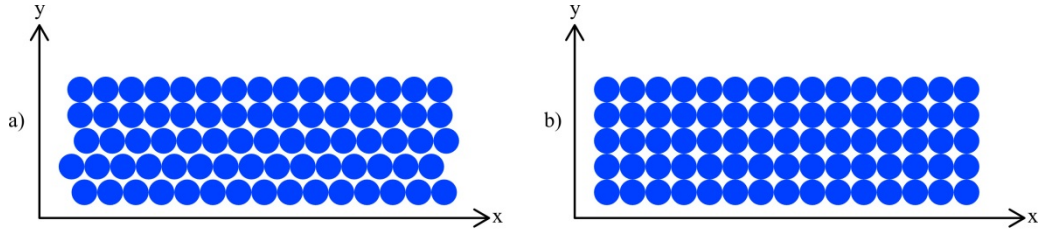


Figure 2. Line position patterns of raster scanning in a) unsynchronized and b) synchronized operation

3. ENHANCED PRECISION IN SYNCHRONIZED GALVO SCANNER OPERATION

Further investigations showed that in synchronized mode a line start error δx and an error δl in the line length depicted in figure 3 persist.

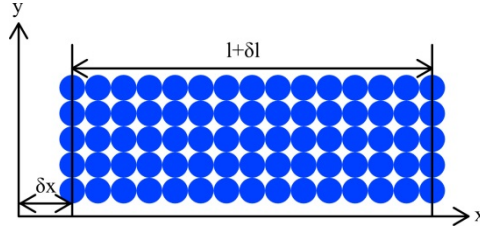


Figure 3. Position errors in synchronized galvo scanner operation.

3.1 Error in line length

In order to understand the causes of the line length error δl the scanner controller operation has to be considered first. Linear scanner movements are parameterized by start and end positions plus the scanner velocity. For a given pitch δ and *PRF* the scan velocity v is

$$v = \delta \cdot PRF . \quad (1)$$

On the other hand the line length corresponds to n equidistant laser pulse positions. Therefore the line length is

$$l = (n - 1) \cdot \delta . \quad (2)$$

Furthermore the scanner evaluates the position at discrete time steps according to the CCF .

$$\Delta t = 1/CCF. \quad (3)$$

In consequence the scanner position is evaluated at discrete time steps $k\Delta t$ with k as a natural number.

$$x(k\Delta t) = v \cdot k\Delta t + x(0) = \frac{v}{CCF} \cdot k\Delta t + x(0) = \delta \cdot \frac{PRF}{CCF} \cdot k\Delta t + x(0). \quad (4)$$

For an arbitrary number of laser pulses and a given scanner velocity the line length l does not necessary match a controller sample position $x(k\Delta t)$. This conflict finally leads to the line length error δl . However this error is removed when the scanner is parameterized with a line length rounded up to the next controller sample position.

$$l_{sc} = \left\lceil \frac{(n-1)}{PRF/CCF} \right\rceil \cdot \frac{PRF}{CCF} \cdot \delta. \quad (5)$$

The actual line length is attained by omitting the supplementary pulses. Figure 4 represents an example situation for $PRF=3 \cdot CCF$, $n=8$ and thus the line length $l=7 \cdot \delta$. The black circles indicate the positions of the laser pulses. The blue filled circles represent the laser pulses at controller sample positions. In this case and according to equation (5) the line length used for scanner parameterization is $9 \cdot \delta$. As mentioned above and indicated by the thin black circles the actual line length l is attained by processing the first 8 pulses only.

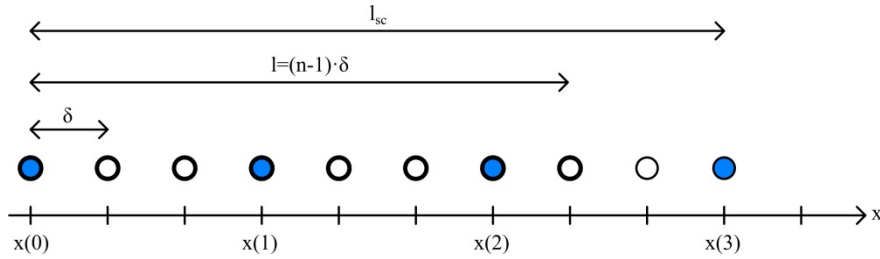


Figure 4. Positions of laser pulses and scanner controller sample positions for $PRF=3 \cdot CCF$.

3.2 Error in line start position

The typical situation for a line start position error δx is depicted in figure 5 where the green tick marks on the x-axis represent the desired pulse positions and the red circles represent the actual laser pulse positions.

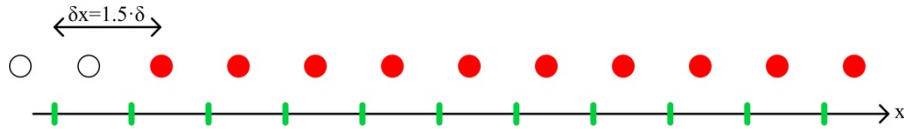


Figure 5. Line start error.

The black circles on figure 5 indicate that the line start error δx can be divided into an integer and a fractional part of the pitch δ . The integer part of the error is removed with a correct laser on delay which in case of figure 5 should start one or two pulses to the left. The remaining fractional part is then reduced by controlling the phase relation between the CCF and the PRF . According to figure 6 a phase control unit is introduced into the controller clock derivation configuration of figure 1.

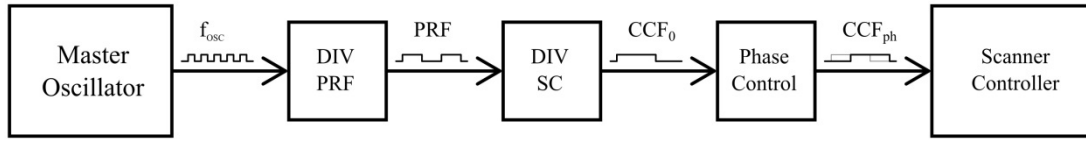


Figure 6. Configuration of clock derivation for synchronized scanner controller operation with phase control of scanner controller clock signal.

The necessary delay and phase settings are determined with the test pattern depicted in figure 7. The lines are processed from left to right at a scan velocity of 1.8m/s. Because of the spot diameter of approximately $10\mu\text{m}$ pulse overlapping is avoided by marking only every seventh pulse. In combination with a pitch of $6\mu\text{m}$ the indicated distance of $42\mu\text{m}$ between two laser marks is obtained. The even lines represent reference positions machined with static galvos and the odd lines represent the positions marked with moving galvos. Compared to the red reference line in figure 7a the position error is $15\mu\text{m}$ or $2.5\cdot\delta$, respectively. In figure 7b the integral part of the error is removed with a laser on delay enabling laser processing two pulses earlier. The fractional part is finally removed by setting the phase offset to π .

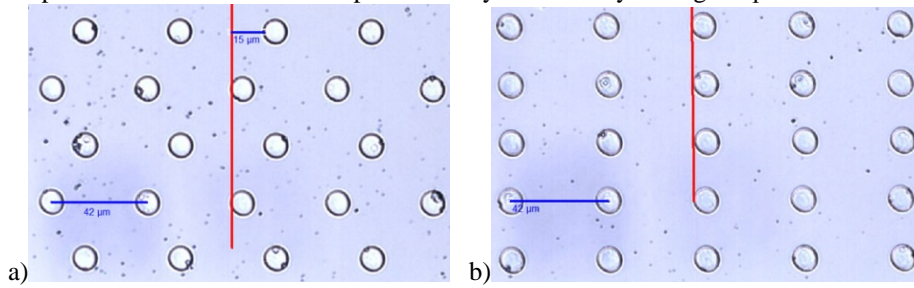


Figure 7. Test pattern with every seventh pulse machined on a silicon waver at $PRF=300\text{kHz}$ and with $\delta=6\mu\text{m}$, a) Initial test pattern with arbitrary laser delay and zero phase, b) Test pattern with adjusted laser delay and phase.

4. BIDIRECTIONAL PROCESSING

So far the laser pulses were only emitted when the direction of scanner movement was in positive x-direction. The grey lines in figure 8 describe the beam trajectories in x-y coordinates for unidirectional processing mode and bidirectional processing mode respectively.

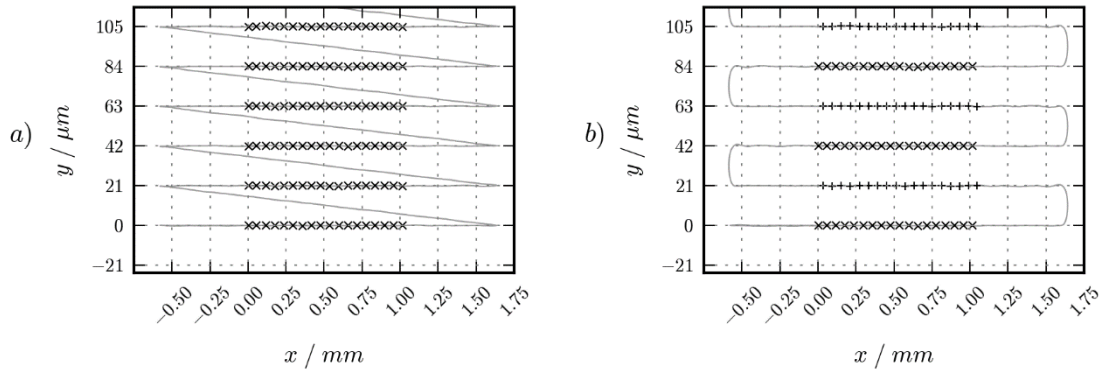


Figure 8. a) Laser beam trajectory in unidirectional mode, b) Laser beam trajectory in bidirectional mode.

Because of physical limits the jump speed of galvo scanners is comparable to marking speed at high speed operation. Therefore the necessary time for the return movement indicated by the oblique part of the trajectory in figure 8a is similar to the process time and consequently the duty cycle of laser operation is inherently low. Adopting a bidirectional processing mode increases the duty cycle of laser operation. The challenges of high precision bidirectional processing are accurate line lengths and accurate line start positions in both scanning directions. Fortunately the proceeding

described in the previous paragraph enables the necessary precision. In fact for bidirectional processing only distinct parameterizations for laser on delay and phase setting in both directions are necessary.

A successful implementation of the calibration process in bidirectional mode is shown in figure 9. The clear dots represent the reference points marked with steady galvos. The checkerboard pattern is marked with a pitch of $3\mu\text{m}$ and a laser frequency of 200 kHz. In order to avoid overlap only every seventh pulse was marked. Therefore the distance between two spots is $21\mu\text{m}$.

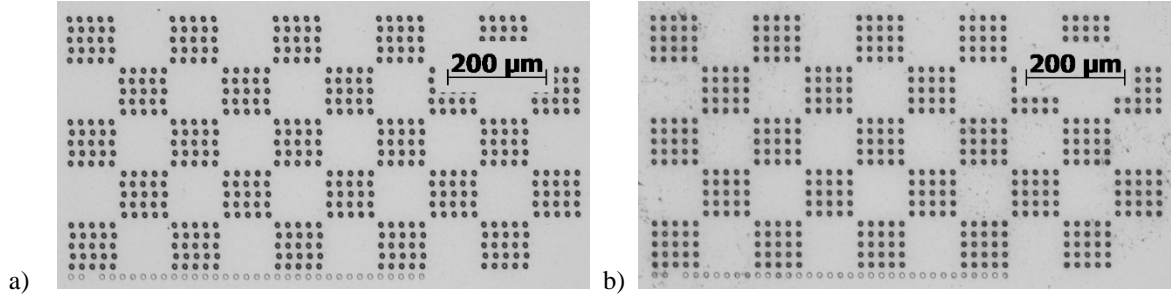


Figure 9: a) Checkerboard test pattern before delay and phase settings, b) Checkerboard test pattern with adjusted delay and phase settings.

By using bidirectional processing the necessary time to machine a 10×10 mm area with a pitch of $3\mu\text{m}$ and a pulse repetition frequency of 200kHz was reduced to 64 seconds. Compared to the 138 seconds required by the setup presented in⁴ the necessary time was roughly divided by a factor of two. Figure 10 depicts a detailed view of a structured surface derived from a grayscale image.



Figure 10. Detail of machined grayscale image⁶. Parameters: $\lambda=532\text{nm}$, $\delta=3\mu\text{m}$, $PRF=1\text{MHz}$, average laser power 1.2W, image size 512×512 points or $1.5 \times 1.5\text{mm}$, process time for one layer 1.2s, overall process time 2min

5. POSITION MEASUREMENT

Both, high precision unidirectional and bidirectional processing modes require accurate delay and phase settings. One possible way is to assess the position error by means of optical microscopy. However this process is time-consuming and difficult to automate. A simple on target and possibly automatable position measurement process is therefore a considerable advantage compared to optical measurements. In consequence the apparatus and proceeding shown in figure 11 were developed.

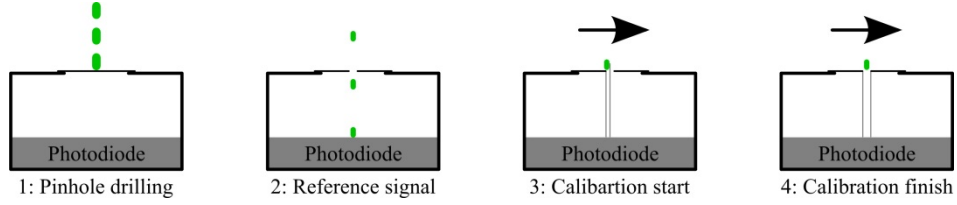


Figure 11: Position measurement apparatus and proceeding

The apparatus is nothing else than a simple photodiode installed in an opaque enclosure. In line with the photodiode a thin metal sheet covers an aperture in the enclosure. The position measurement proceeding is divided into three main steps. The first one consists in drilling a pinhole with static galvos into the metal sheet at the desired reference position. Subsequently laser pulses are sent through the pinhole and captured by the photodiode. The photodiode current is amplified and transformed into a voltage signal with a transimpedance amplifier. The evolution of the resulting voltage signals is depicted in figure 12. In dynamic mode the alignment between the laser pulse and the pinhole is achieved when the both diode signals have an identical shape.

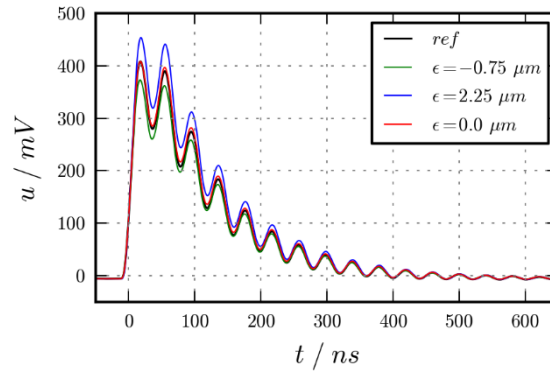


Figure 12. Photodiode voltage signals at $v=1.5\text{m/s}$, $\delta=3\mu\text{m}$ and $PRF=500\text{kHz}$

The black curve in figure 12 represents the voltage signal obtained with static galvos. The blue and green curves represent voltage signals when the integral part of the line start error is equal to zero. Finally the red curve represents the diode signal with a minimized position error. The position measurement was successfully tested at 1064nm, 532nm and 355nm wavelength. The practical resolution depends on the spot size and is in the range 0.05 to 0.1 times the spot size. Hence for a spot size of $5\mu\text{m}$ the practical accuracy is in the range $0.25\mu\text{m}$ to $0.5\mu\text{m}$. In future work this device will also be used for position measurement with polygon mirror scanners.

6. COMBINATION WITH MECHANICAL AXES

Commercially available galvo scanner systems have a scan area of about $40\times 40\text{mm}$ by using a 100mm objective. In combination with one high precision linear axis it is possible to enhance the working field as shown in figure 13.

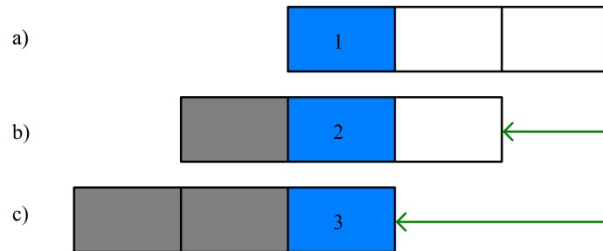


Figure 13. Combination of scanner working areas with one linear additional linear axis. a) First working field, b) second working field, c) third working field

In order to achieve high precision alignment of the adjacent working fields the exact relations between the scanner coordinate system and coordinate system of the linear axis have to be measured. In combination with the previously presented measurement system the procedure depicted in figure 14 was used to measure the angle α between the linear axis- and the scanner-coordinate system.

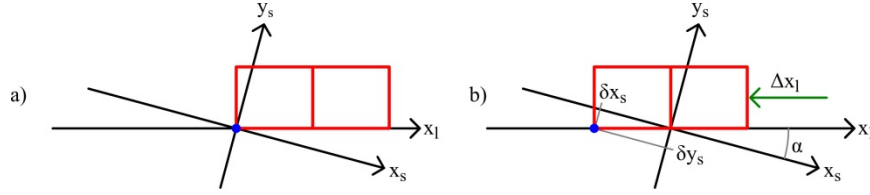


Figure 14. Measurement of angle and stretch between linear axis coordinate system (l) and scanner coordinate system (s) a) Definition of reference position pinhole, b) Displacement of work piece with linear axis and subsequent measurement of position in scanner coordinate system.

First of all a pinhole is drilled at the designated origin of the two coordinate systems. Hereafter the pinhole and hence the origin of the linear axis coordinate system is displaced by Δx_l with the linear axis. Finally the scanner is used to search the location $(\delta x_s, \delta y_s)$ of the pinhole in the scanner coordinate system. The angle α between the two coordinate systems is equal to

$$\alpha = \arctan\left(\frac{\delta x_s}{\delta y_s}\right). \quad (5)$$

And the displacement in the scanner coordinate system is equal to:

$$\Delta_s = \sqrt{\delta x_s^2 + \delta y_s^2}. \quad (6)$$

The length Δx_l is determined by the linear axis encoder and the length Δ_s is determined by the scanner encoders. Due to tolerances a small error between these two line lengths is inevitable. If this error is not compensated a gap between two adjacent working fields subsists. Therefore the pitch in scanner coordinates is adapted according to

$$\delta_s = \frac{\Delta_s}{\Delta x_l} \delta_l. \quad (7)$$

Figure 15 depicts the results with the previously used checkerboard structure.

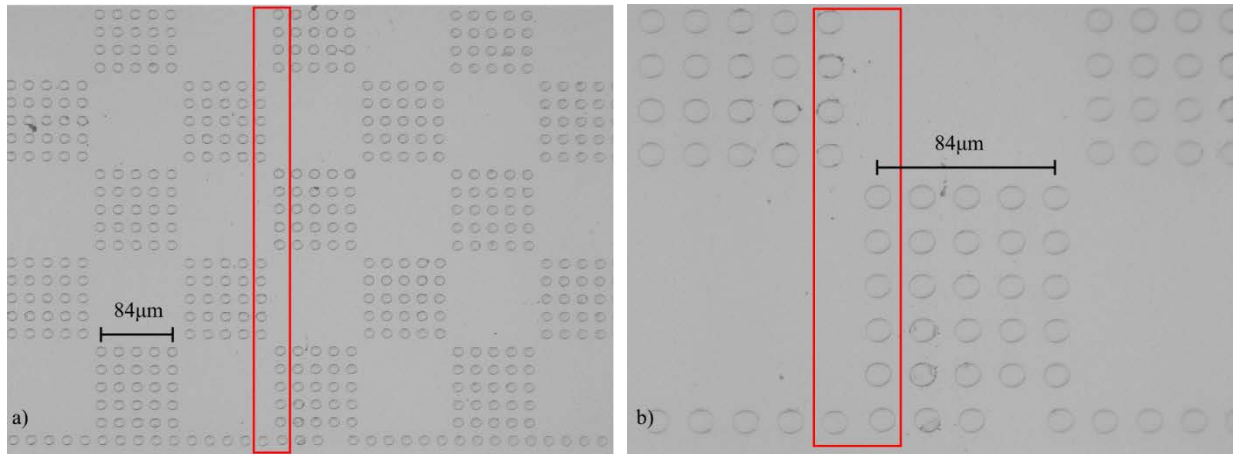


Figure 15. a) Adjacent of working fields, b) detailed view of adjacent working fields

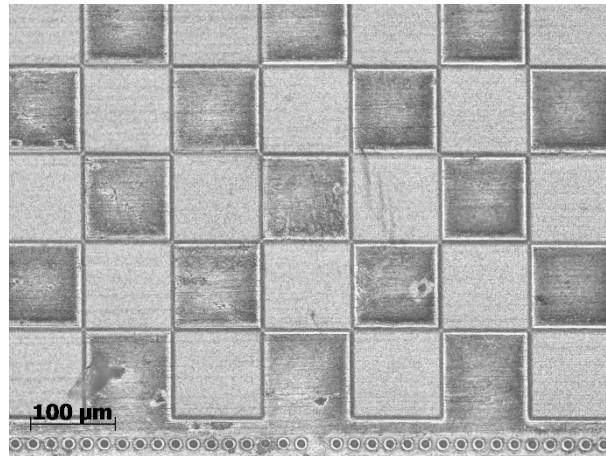


Figure 16. Machined checkerboard structure. The transition is located left to the missing dot in the reference line.

7. CONCLUSION AND OUTLOOK

The presented improvements in high precision galvo scanner micromachining represent a major step towards industrial applications. A successful implementation of high precision bidirectional scanning mode was presented. The presented method for position measurement was used for the parameterization of the scanner system and for adjustment with an additional mechanical axis. A scanner with an optimized galvo tuning is currently tested. The first test results are very promising as a precision in the range of $\pm 2\mu\text{m}$ at scanning velocities beyond 20m/s seem to be possible.

8. ACKNOWLEDGEMENT

This work was supported by the European Union in the FP7 project APPOLO.

REFERENCES

- [1] Raciukaitis G., Brikas M., Gecys P., Voisiat B., Gedvilas M., "Use of High Repetition Rate and High Power Lasers in Microfabrication: How to keep Efficiency High?", JLMN Journal of Laser Micro/Nanoengineering Vol. 4 (3), 186-191 (2009)
- [2] Neuenschwander B., Bucher G., Hennig G., Nussbaum C., Joss B., Muralt M., Zehnder S. et al., "Processing of dielectric materials and metals with ps laserpulses," ICALEO 2010, Paper M101, (2010)
- [3] Neuenschwander B., Bucher G., Nussbaum C., Joss B., Muralt M., Hunziker U. et al., "Processing of dielectric materials and metals with ps-laserpulses: results, strategies limitations and needs," Proceedings of SPIE Vol. 7584, (2010)
- [4] Jaeggi B., Neuenschwander B., Hunziker U., Zuercher J., et a., "Ultra high precision surface structuring by synchronizing a galvo scanner with an ultra short pulsed laser system in MOPA arrangement", Proceedings of SPIE Vol. 8243, (2012)
- [5] Neuenschwander B., Jaeggi B., Zimmermann M., Penning L., De Loor R., Weingarten K., Oehler A., "High throughput surface structuring with ultrashort pulses in synchronized mode with fast polygon line scanner", ICALEO 2013, Paper M203, (2013)
- [6] <http://en.wikipedia.org/wiki/Lenna#mediaviewer/File:Lenna.png>